GROWTH MECHANISMS AND POLYTYPISM IN SYNTHETIC HYDROXYL-BEARING PHLOGOPITE

A. Baronnet, *Laboratoire de Minéralogie et Cristallographie et Laboratoire des Mécanismes de la Croissance Cristalline associé au C. N. R. S., Université de Provence, Saint Jérôme, 13 Marseille 13ème, France*

Abstract

Self-nucleated and hydrothermally grown minute phlogopite crystal populations have been studied by electron microscope. Growth by Frank's spiral mechanism is observed after an initial growth by a layer mechanism. Different types of spirals and their interactions have been analyzed and correlated with polytypism in this mineral. Two different basic structures of layer–growth $1M[0]$ and $1M_r n(120)$ have been directly identified.

Introduction

In order to gain a better understanding of the correlation between polytypism and growth mechanisms of micas, a statistical study of crystallites, as suggested by Smith and Yoder (1956), may give more precise information than the previous studies of Amelinckx (1952a), Amelinckx and Dekeyser (1953), Sunagawa (1964), and Kretz (1966): these authors were working on well-developed natural specimens grown at low supersaturations and showing only the late-growth features on (001) faces.

The more interesting observable phenomena connecting growth mechanisms with polytypism are encountered in the first stages of crystal growth. With that in mind, we have performed a careful microtopographic study on crystallite populations of controlled chemical composition and growth conditions. In order to describe the time evolution of the surface structure from a single specimen, we have followed this evolution on a series of crystallite populations with increasing run durations, rapidly quenched from hydrothermal growth experiments. Later on we will be able to define a "representative crystal" from each population showing the statistically dominant growth features and consider the implications of its microtopographic evolution on the crystal structure.

This study was carried on hydroxyl–bearing phlogopite, a mineral of common occurrence in ultrabasic igneous rocks and in marbles.

Synthesis and Growth Conditions

Phlogopite synthesis and growth are carried out in sealed gold tubes held in "cold seal" pressure vessels (Tuttle, 1949). Pressure is applied by an isostatic pump and the desired temperature is obtained by external heating of the vessel.

Pressure rise with time in the gold tube during temperature rise of the vessel is achieved in such a way that, in all the runs, the internal volume expansion of the tube is always reproducible. This careful regulation is necessary to obtain good reproducibility of the results between different runs at identical final P and T.

The initial material is a stoechiometric mixture of K, Al, and Mg nitrates mixed with high purity amorphous silica. The mixture is heated up to $500°C$ during two hours to remove most of the NO_2 (Roy, 1956). The resulting powder is ground and used as the starting charge. All the crystalline populations are grown under the following conditions: amount of starting charge, 25 mg; weight of doubly distilled water, 100 mg; temperature $600 \pm 2°C$; pressure 1020 ± 34 bars; axial thermal gradient along the gold tube $\simeq 2–3°C/cm$; gold tube length, 30 mm. The only variable is the run duration t; the origin of time t_0 is taken at the moment when P and T in the vessel reached stationary values, i.e., 90 minutes after the vessel is inserted in the furnace. The chosen t values are: $t_1 = 10$ minutes; $t_2 = 1$ hour; $t_3 = 3$ days; $t_4 = 15$ days; $t_5 = 30$ days.

Methods Employed for the Microtopographic Study

At the end of a run, the crystalline power is spread on thin glass microscope slides and then submitted to platinum/carbon shadowing, gold flash evaporation and impurity decoration.

Platinum/carbon shadowing. When the best contrast conditions are realized, this method is capable of a resolution of about 10 Å, *i.e.*, the height of a elementary mica layer.

Gold flash decoration. This technique (Bassett, 1958; Sella, Conjeaud and Trillat, 1960), first applied on clay minerals by Gritsaenko and Samotoyin (1966), allowed them to decorate small details of surface microtopography of the order of atomic size. The following optimum predecoration treatment was used for the case of hydroxyphlogopite: heating temperature, 300–550°; heating times, 45–90 minutes; temperature of the crystals during the decoration, 150–180°C; vacuum: $1 \times 10^{-5}–8 \times 10^{-6}$ Torr.

For the special purpose of step-height measurements, an inclined gold vapor beam was used for the decoration. Natural (Sunagawa, 1964) and synthetic (this work) phlogopite frequently shows selective precipitation of impurity crystals along growth steps which block a part of the chemically and energetically most active regions; therefore, continuous step decoration is difficult to obtain without using very high heating temperatures.

Impurity decoration. In order to prevent the above disadvantage, a special decoration technique was used. After spreading the crystals on the glass slide as mentioned before, they are immersed under a thin layer of a dilute solution of potassium nitrate that is then evaporated very rapidly, followed by platinum/carbon shadowing. The potassium nitrate crystallites nucleate with the greatest density at the growth steps. Micrographs obtained by this technique are shown in Figures 2d, 15, and 17.

TABLE 1. Relative growth feature frequencies on (001) as a function of run durations: strong $++$, mean $+$, weak $(+)$, frequencies; 0—missing.

Type I runs: $1M$[O] polytype

t	Smooth face	Growth islands	Steps	Spirals A	Spirals B	Spirals C
10 minutes	$++$	$(+)$	$(+)$	0	0	0
1 hour	$+$	$(+)$	$+$	0	0	0
3 days	$(+)$	0	$++$	$+$	0	0
15 days	$(+)$	0	$(+)$	$+$	$++$	0
30 days	$(+)$	0	$(+)$	$+$	$++$	0

Type II runs: mixture of polytypes						
15 days	$(+)$	0	$(+)$	$+$	0	$++$

TOPOGRAPHIC EVOLUTION OF {001} FACES

The following growth patterns were distinguished on {001} faces:

—growth islands: incomplete layers bounded by a closed step.
—growth steps: steps running across {001} faces but not belonging to spiral growth fronts.
—spirals with an undissociated growth step; elementary spirals or spirals originating from dislocations of multiple strength (type A).
—spirals with their exposed edges dissociated into several component steps. Two cases are found on phlogopite:
   a) the successive component sheets are described by polar diagrams of the same form and orientation (Figures 2b, c, d). This kind of spiral may be considered as a cooperating spiral group (type B).
   b) if the growth rate of a sheet depends on crystallographic directions and if the orientation of such a growth unit is different from the neighboring ones, interlaced spirals arise (type C).

These spirals are intimately connected with polytypism: Verma (1951, 1952, 1953); Frank (1951a).

Table 1 plots frequencies of growth features observed, against run durations. During the first stages of growth ($t_1 = 10$ minutes, $t_2 = 1$ hour), {001} faces are smooth, with occasionally one or two growth steps (Fig. 1a). Approximately polygonal islands are seen on the smallest crystallites (inset Fig. 1a); the growth of {001} faces proceeds by a secondary nucleation mechanism. For three day-experiments (Fig. 1b), exposed ledges were observed for the first time (inset Fig.
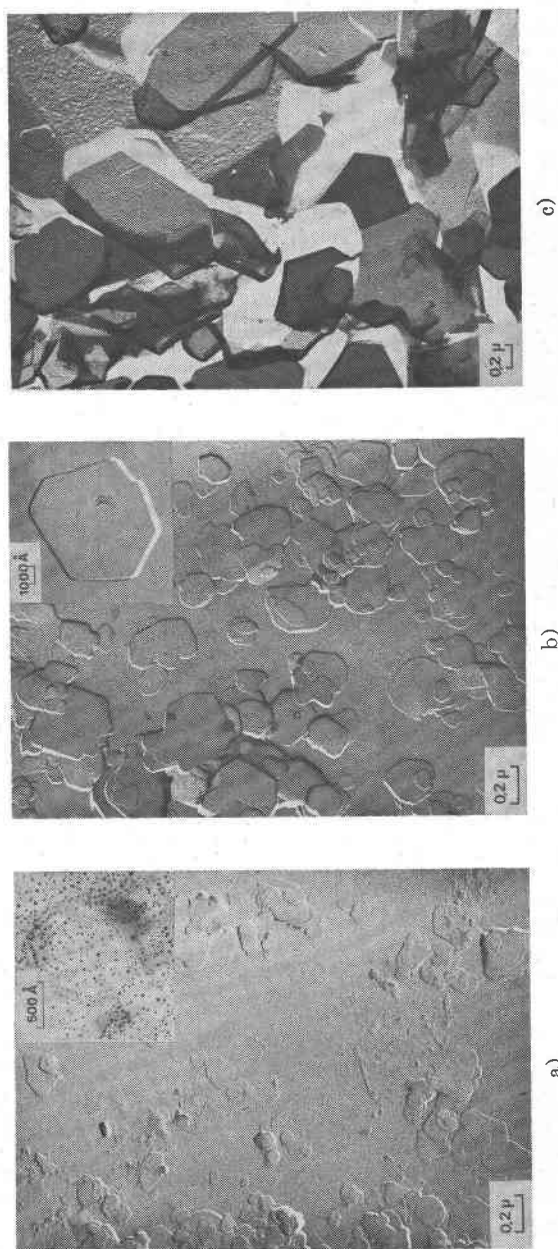
FIG. 1. Phlogopite crystal populations grown at $T = 600°C$ and $P = 1$ kbar for (a) 10 minutes, (b) 3 days, (c) 15 days.

1b). In 15- and 30-day experiments, spirals are common on basal faces (Fig. 1c, 10, and 18).

GROWTH SPIRAL ANALYSIS

Among the 30 different runs of 15 days made, the great majority exhibited only type A and B spirals: they are called type I runs.

Type I Runs: 1M [0] Polytype

The changing symmetry, morphology, and degree of polygonization of growth fronts, Burgers vector values of screw dislocations which may or not have a hollow core, are among the many observed characteristics of the growth spirals.

Morphology and symmetry of growth fronts. The two most frequent shapes are shown in Figures 2a and 2c. The simultaneous observation of the crystal morphology allows the indexing of the rectilinear parts of growth fronts, as (a) in Figure 2a, two spirals of opposite sign with pseudohexagonal fronts, [100], [1$\bar{1}$0], [110]; and (b) in Figures 2c and 2d, a rectangular [010] and [100] pattern of apparent $2mm$ symmetry with more or less curved corners. Straight lines along [100] are always the longest, *i.e.*, their rates of growth are the slowest. This is in good agreement with Sunagawa's (1964) observations on natural phlogopite, but in contrast to his work I found no five–sided spirals. The five-sided morphology might be a combination of the above two forms. The correlation, between the most frequent front directions and the directions of relatively close packing of oxygen ions in the structure, that was pointed out by Kretz (1966) is verified, but the domination of [010] over [3$\bar{1}$0] and [310] is not explained.

Growth spiral and growth pattern forms are not always closely connected with those of crystal edges bounding {001} faces (Figure 2a, b, c, d) as described for apatite by Amelinckx (1952b) and for other compounds by Brandstätter (1952, 1953).

On a given crystal, the morphology of the successive fronts of a spiral originating from a dislocation group (Fig. 2b, c, d) doesn't depend on their respective height.

Spiral polygonisation. A study (Baronnet) of the time variation of supersaturation near the crystals shows that it is a decreasing function of run duration; the degree of polygonisation also decreases with time [Fig. 2a ($t_4 = 15$ days); Fig. 6a and 6b ($t_5 = 30$ days)]. As the growth temperature is the same in all the experiments, the more or less polygonised nature of spirals may be related to variations of supersaturation and consequent changes in the critical nucleus size.

Measurements of spiral step heights. Measurements of growth step heights and of the c^* component of Burgers vector $\bar{b}$ of a spiral is possible
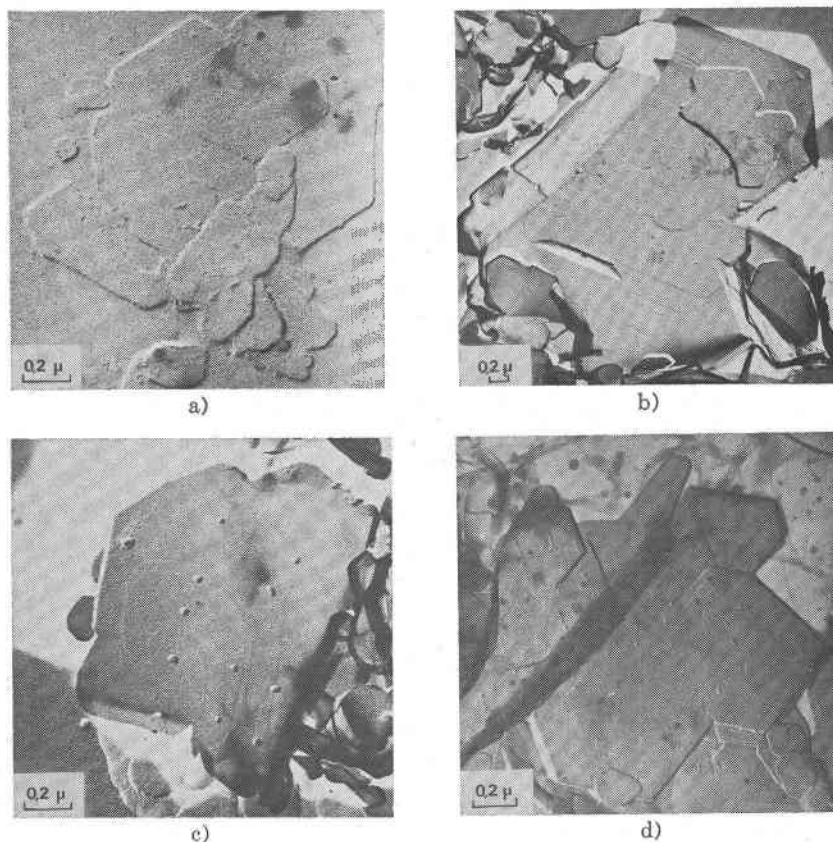
FIG. 2. Different spiral types observed on $1M(0)$ polytype (type I runs): a). two growth spirals of opposite sign with pseudohexagonal growth fronts; b). pseudohexagonal spiral group starting from a hollow dislocation; c). Rectangular spiral growth fronts with curved corners; and d). Rectangular spiral group "dominating" two spirals of opposite hand.

for a small number of microtopographic configurations (See Figs. 3 and 4). A vicinal face created by equally spaced steps on (001) appears on a crystal laying flat on the glass slide. A part of the step G to be measured also belongs to the vicinal face: then, the mean height of the close spaced steps $(h)_{m0}$ can be calculated:

$$(h)_{m0} = \frac{H_1 - H_2}{gn \tan \alpha}$$

where:

H_1 and H_2 are two shadow lengths measured along the gold vapor beam direction,
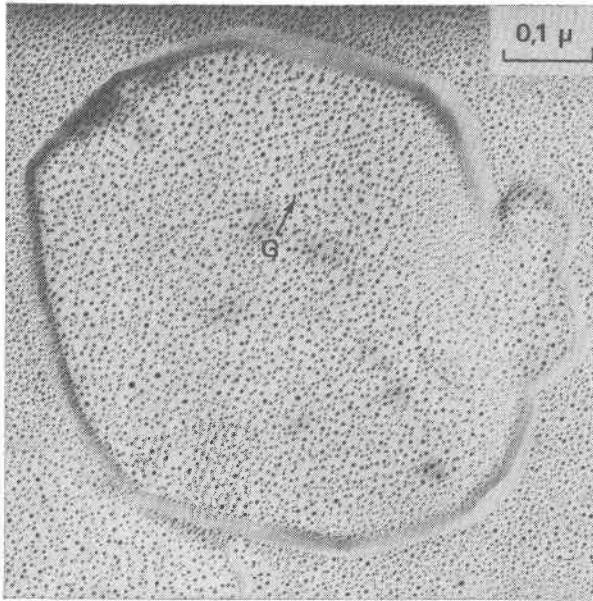
FIG. 3. Inclined gold-decorated microtopographic configuration permitting the height measurement of the growth step G.

n, is the number of steps existing between the 2 points of measurements of H_1 and H_2,

g, is the magnification of the micrograph, and

α, is the inclination angle of the gold vapor beam during the decoration. For measurements on ten vicinal faces we obtain $9 \text{ Å} < (h)_{m0} < 11 \text{ Å}$, *i.e.*, all steps constituting a vicinal face are monomolecular and G is a monolayer growth step (Fig. 3). In Figure 5, a spiral step is split into three monomolecular steps, *i.e.*, the c^* component of the Burgers vector of the screw–dislocation is 30 Å; values of 10, 20, 60, and 120 Å were found on other crystals.

Hollow dislocations in phlogopite. At the point of emergence of screw dislocations of multiple strength on {001}, empty tubes are commonly observed if the Burgers vector exceeds a critical value of approximately 20–40 Å. In good agreement with Frank's work (1951b), the diameter D of the tube is an increasing function of $\bar{b}$ (see Figs. 6a and 6b). In Figures 2b, 8, 9, 10, and 15 other hollow cores appear. They certainly play an important part in the trapping of crystalline impurities during the growth of mica crystals.

Interactions of growth spirals. Hydroxyl–bearing phologopite exhibits

classic interaction patterns previously seen on other compounds (Verma, 1953; Dekeyser and Amelinckx, 1955), such as:

—two spirals of opposite hand, initiating a closed loop in Figure 7a. A large growth front between unlike dislocations is divided into several component steps in Figure 7b.

—two cooperating spirals of the same hand in Figure 9c; the growth ledges are moving around the two hollow dislocations, which are linked by a large step.

—spiral group patterns originating from four dislocations of multiple strength are shown in Figure 7d. A curious phenomenon, shown by arrow in this figure occurs frequently on phlogopite, where a spiral growth front is overlapping with another spiral and, in spite of that, remains undisplaced. The screw dislocation line should escape the crystal by running into one or several edge dislocation lines emerging on vicinal or on natural prismatic faces (Fig. 8). Let b_s be the Burgers vector component along c^* of the overlapped screw–dislocation and b_e, the
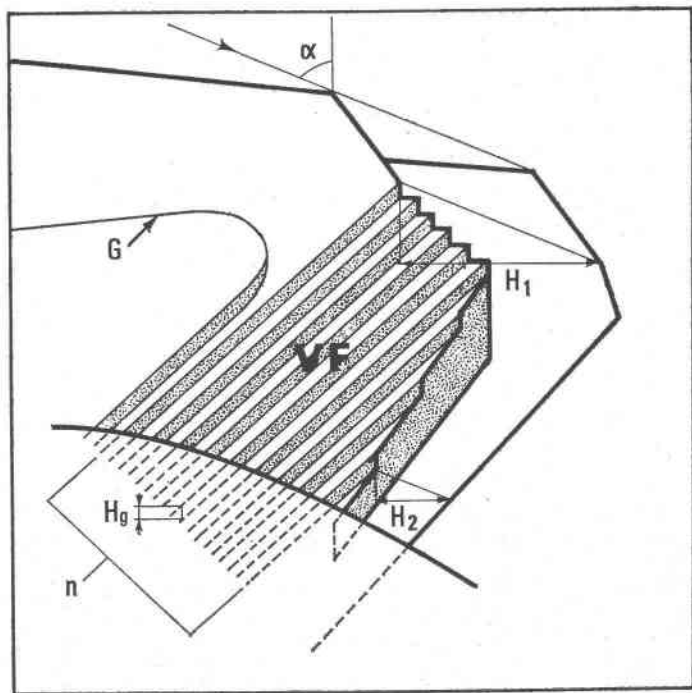
FIG. 4. Schematic illustration of the configuration of the upper right part of the crystal shown in Fig. 3.
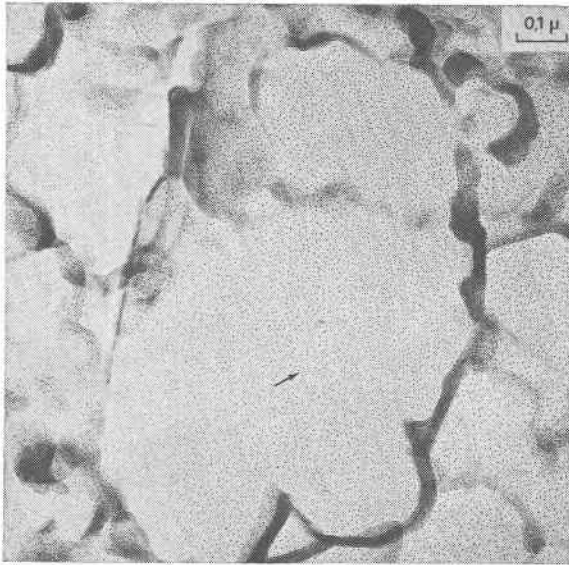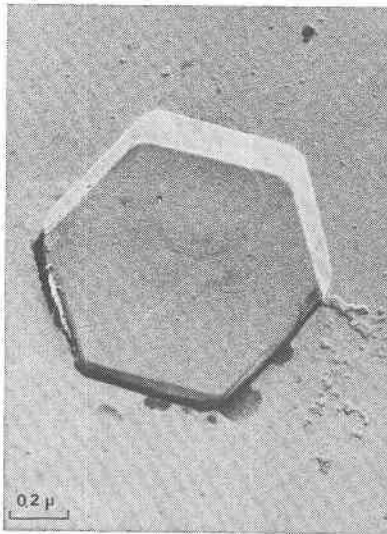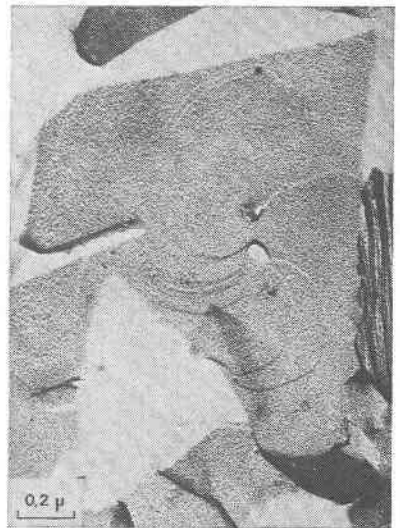
Fig. 5. Gold-decorated (001) face showing a 30 Å spiral.

a)

b)

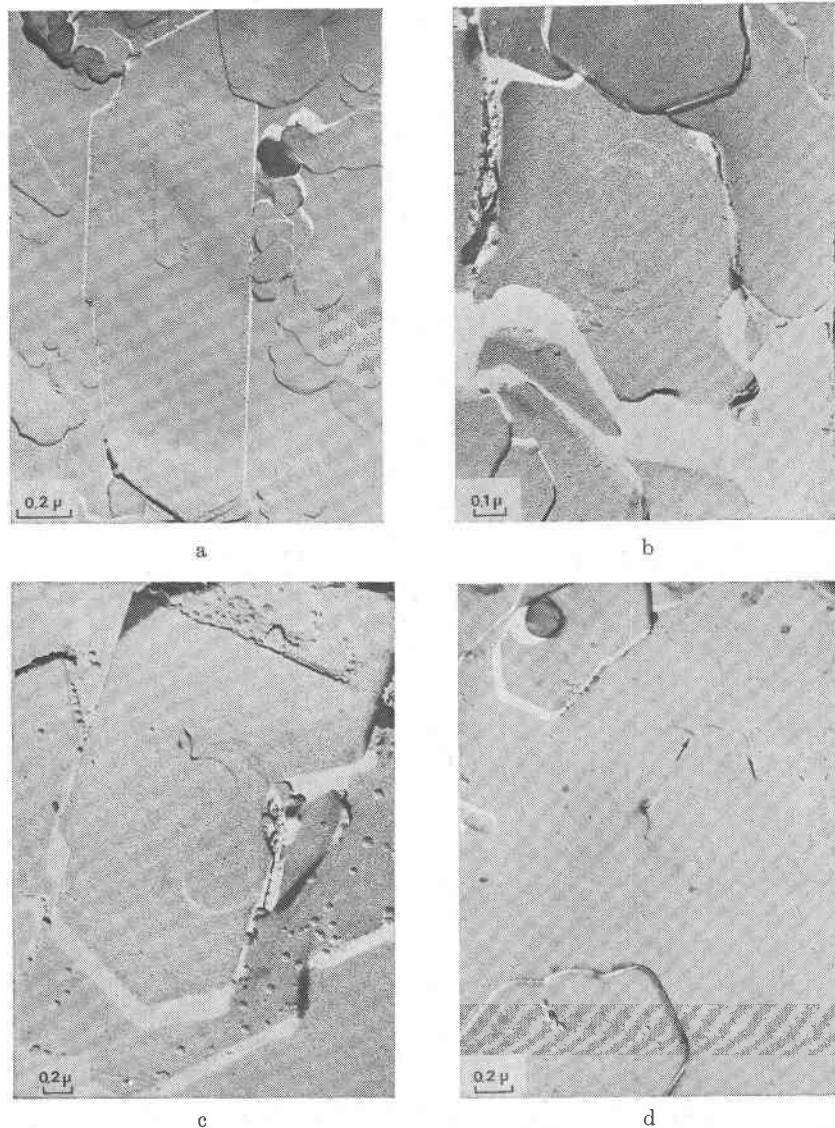Fig. 6. Hollow screw dislocations with (a) small and (b) large Burgers vectors.

Fig. 7 a. Two screw dislocations of opposite hand linked by a single growth step
($|\mathbf{b}_1| = |\mathbf{b}_2|$ for small **b**'s).

b. Two screw dislocations of opposite hand linked by component steps
($|\mathbf{b}_1| = |\mathbf{b}_2|$ for large **b**'s).

c. Cooperating spirals of the same hand; a large step links the two
dislocation cores

d. Numerous spirals on the same crystal: the arrow shows a screw dislocation
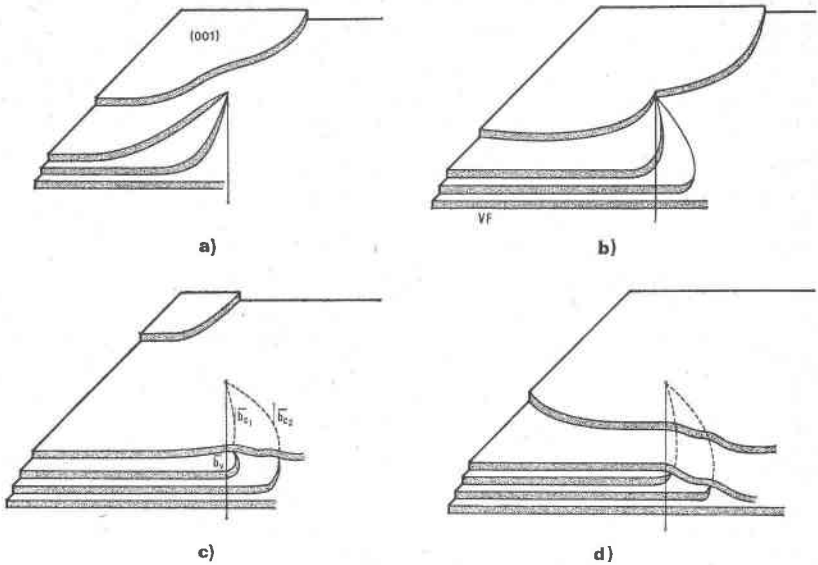core with an overlapping spiral growth front.

FIG. 8. Schematic illustration of a screw dislocation line escaping a crystal, and then generating one or several edge dislocation lines during the growth of a mica crystal.

Burgers vector of the ith among the j edge dislocations created by the "old" spiral, then we have:

$$\mathbf{b}_v = \sum_{i=1}^{i=j} \mathbf{b}_{ci}$$

This is the energetically more acceptable mechanism explaining the formation of frequent edge–dislocations seen on vicinal faces; in Figure 9 two edge dislocations of opposite sign with 20 and 10 Å Burgers vectors are visible by gold decoration.

Type II Runs: Mixture of Polytypes.

Among 15 days experiments, three of them exhibit interlaced spirals. *Interlaced spirals with only one kind of polar diagram.* The great majority of spirals with large **b** show very different stacking sequences of layers from one crystallite to another (Fig. 10).

If **b** is small, interlaced or non–interlaced growth spirals corresponding to the simplest polytypic structures are observed:

—In Figure 11 a single lamella is emerging on (001). The form of the growth front does not depend on its height and, therefore, the corresponding polar diagram has been drawn. It corresponds to the plane

symmetry 2 and the slowest growing front is always [100]. If we assume that the P layers of the lamella are in the same orientation and if we use the Ramsdell notation followed by a Ross–Takeda–Wones Symbol (1966) to describe the successive "interlayer stacking angles" (Smith and Yoder, 1956) of the polytype, we obtain the structure $1M[0]_P = 1M[0]$.

—In Figure 12 two lamellae A and B are distinguished, and the two associated polar diagrams are successively derived from a 120°– or 300°–rotation. As only $k \cdot 120°$ stacking angles, with $k = 0$, 1, or 2, occur in the stacking sequences of natural phlogopite polytypes (Ross, Takeda, and Wones, 1966), the chosen rotation angle between A and B will be 120° and between B and A, 240°. If there are P monolayers in the lamella A, and Q layers in the lamella B, then the polytype will be:

$$(P + Q)M[(0)_{P-1}2(0)_{Q-1}\bar{2}] \quad \text{if} \quad P = Q \quad \text{and}$$

$$(P + Q)T_c[(0)_{P-1}2(0)_{Q-1}\bar{2}] \quad \text{if} \quad P \neq Q.$$

In Figure 12, $P \simeq Q = 1$ or 2, and the spiral growth pattern can be considered as the $2M_1[2\bar{2}]$ polytype.

—In Figure 13 three lamellae A, B, and C composed of P, Q, and R monolayers are generating a periodic succession of stacking angles: $(P - 1) \times 0°; 120°; (Q - 1) \times 0°; 120°; (R - 1) 0°; 120°$. Therefore, the stacking sequence of the polytype is

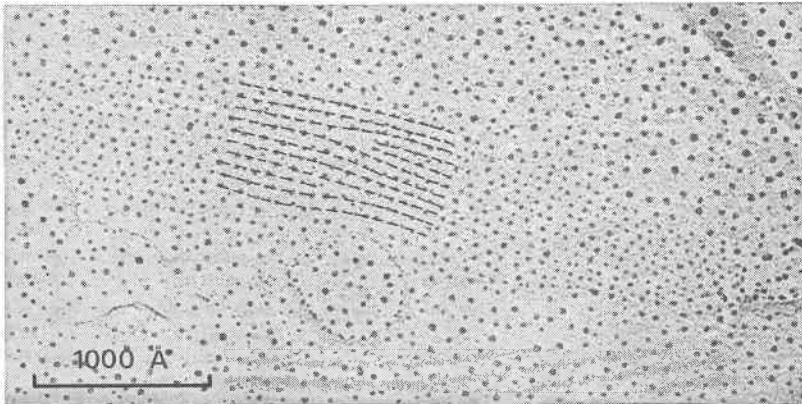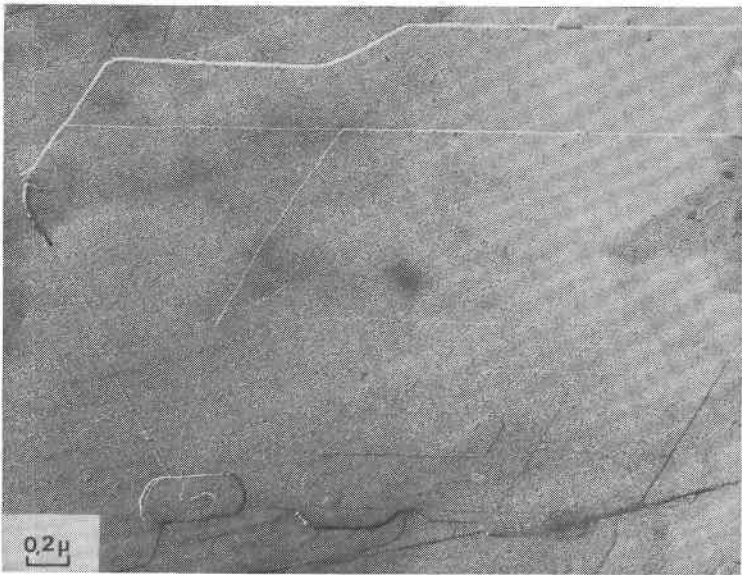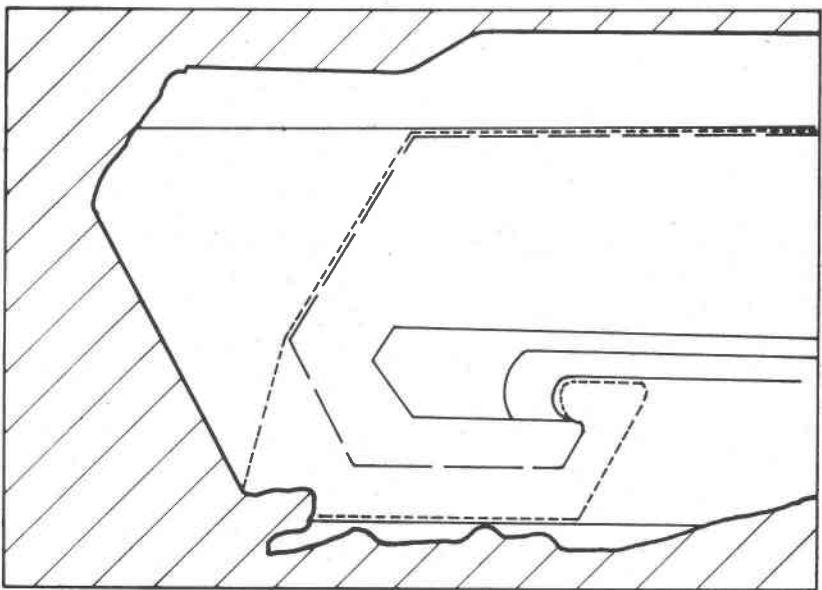$$[(0)_{P-1} 2(0)_{Q-1} 2(0)_{R-1} 2]$$

Fig. 9. Gold-decorated vicinal face exhibiting two edge dislocations of opposite sign.

(a)

(b)

FIG. 10. Complex interlaced spiral appearing on the $1M_rn(120)$ basic structure when the Burgers vector of the screw dislocation is large (type II runs).
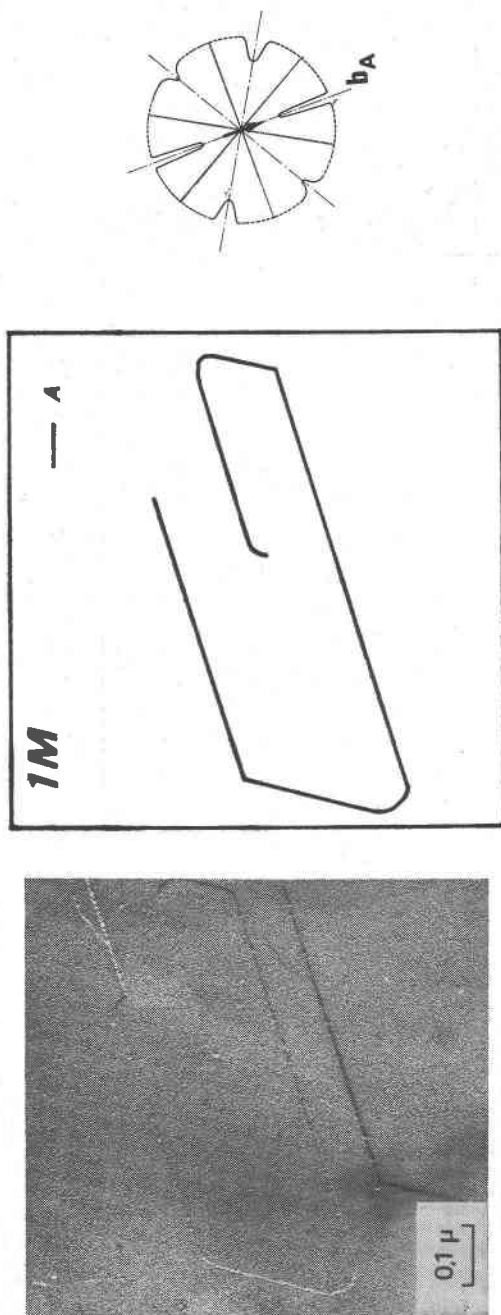
Fig. 11. $1M[0]$ surface structure generated by a spiral appearing on the basic structure $1M.n(120)$. Note the plane symmetry 2 of the growth front.
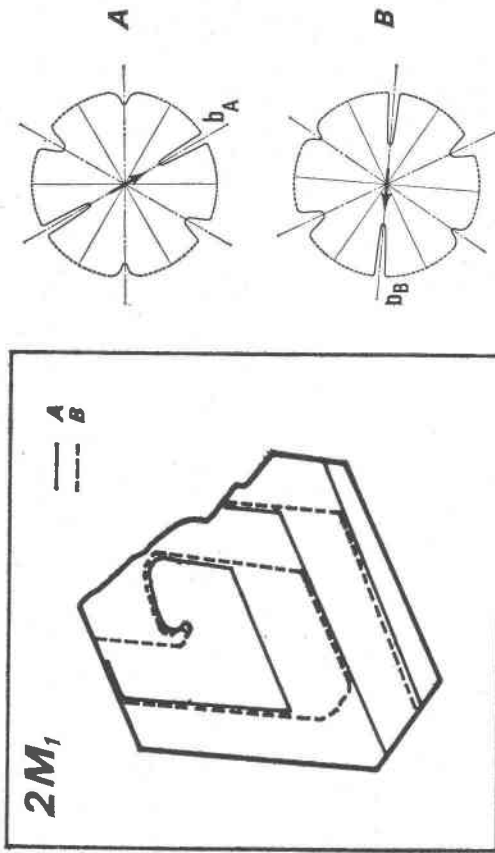
FIG. 12. Spiral growth pattern of the $2M_1[2\bar{2}]$ surface structure on the $1M_{rn}(120)$ basic structure.
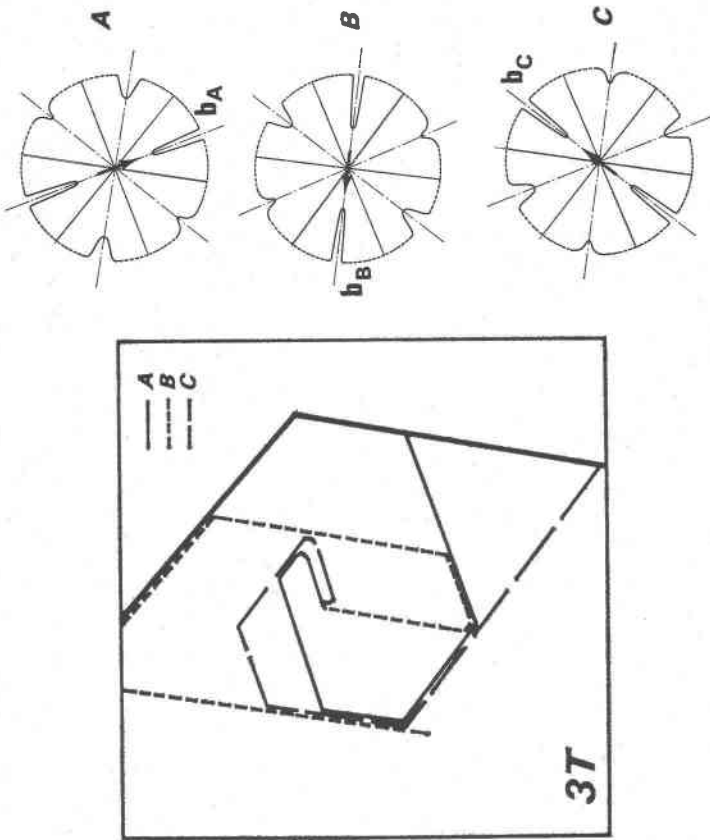
FIG. 13. Spiral growth pattern of the $3T[222]$ surface structure on $1M, n(120)$ basic structure.

If $P = Q = R = 1$, this interlaced spiral is the growth pattern of the $3T$ [222] polytype.

Interlaced spirals with two kinds of polar diagrams. Such spirals are the combination of two polar diagrams of 2 and $3m$ plane symmetries (Fig. 14). If we consider that, (a) the growth conditions are the same for the two fronts, (b) The minimum growth unit in mica is a single sheet of Cm symmetry, (c) Splitting of a spiral growth front occurs if its sequence contains interlayer stacking angles different from 0°, and that the above observations indicate that neither the height nor the orientation of the growth front with respect to the substrate has any significant influence on the shape of the polar diagram, then the reasons for the appearance of this pattern remain unknown.

Interlaced spiral interactions. Figure 15 shows the complex growth patterns occuring with the interaction of several interlaced spirals on a area of one square micron. Notice that when two fronts laying on the same substrate meet others, a residual step (GR) is often observed, revealing their different heights.

Discussion

These detailed observations concerning surface features of basal planes of synthetic phlogopite were carried out in order to discuss the relation between growth mechanism and the origin of the various polytypes of micas. The first ideas along this line were stated by Amelinckx (1952), Amelinckx and Dekeyser (1953), and Smith and Yoder (1956). On one hand, starting from our experiments, nothing can be said about the role of composition and $P–T$ growth conditions of crystals, these factors being maintained constant. On the other hand, the role of growth mechanisms is directly observed. Surface topographies of micas were previously investigated by means of phase contrast and interferometric microscopes by Tolansky (1946a, 1946b) who was working on cleavages, and later by Amelinckx and Dekeyser (1953). Helicoidal surfaces were recognized on muscovite and the first observation of an interlaced growth spiral on a biotite crystal was analysed in great detail and correlated with the polytypism of this mineral. Further investigations on natural crystals showed (Sunagawa, 1964) or did not show (Kretz, 1966) growth spirals; and these authors considered that mica grows either by a spiral growth mechanism or by secondary nucleation of each additional layer. Our investigations make clear that in the first case secondary nucleation is operative before the first screw dislocation appears on the crystallite.
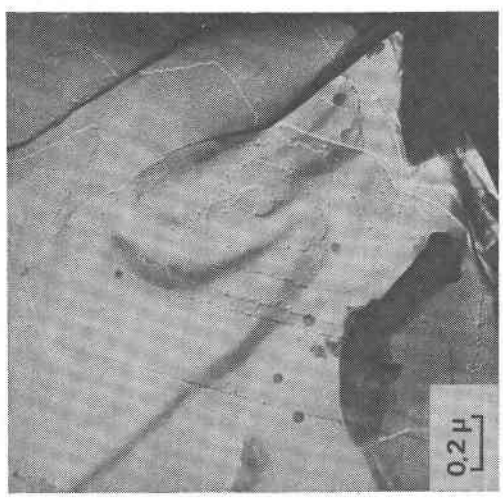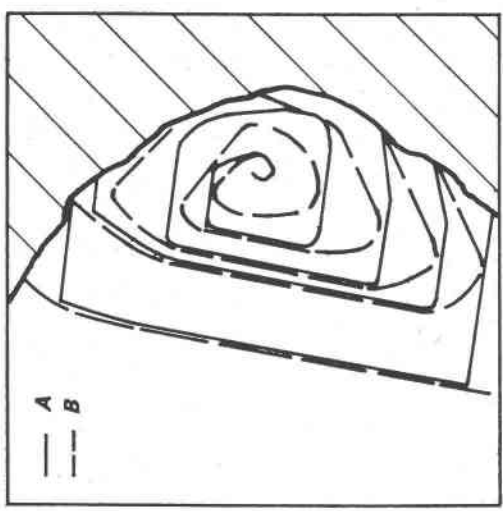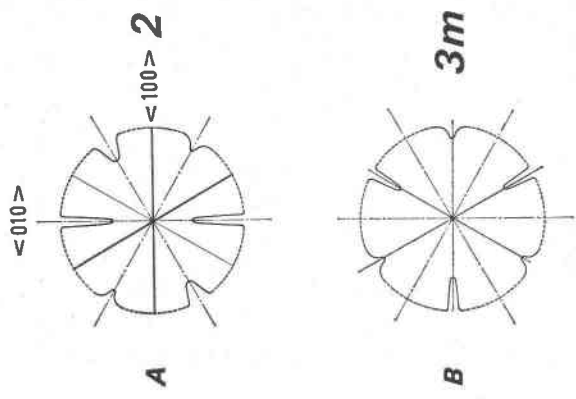
Fig. 14. Interlaced spiral containing two growth fronts of respectively 2 and 3m plane symmetries.
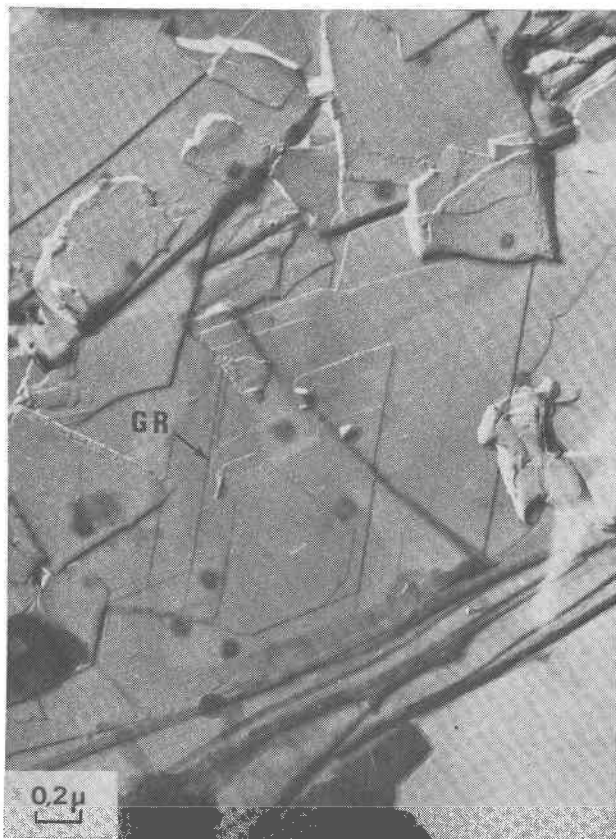
FIG. 15. Interaction of interlaced spirals on $1M_rn(120)$ basic structure.

According to Dekeyser and Amelinckx's ideas, secondary nucleation provides completely random stacking, " . . . There is no reason for a secondary nucleus to adopt a selected orientation on the substrate, the stacking energy differences between the six possible ways of stacking two layers being negligible or zero . . .". If such be the case, the more common $1M[0]$ polytype of phlogopite can only be derived from spirals, the exposed ledges of which do not contain any interlayer stacking angle different from 0°. The *simultaneous* realization of these restrictive conditions, including both the stacking sequence in the exposed ledge and dislocations of very feable strengths on numerous crystals, I consider suspicious.

Smith and Yoder, based on qualitative and semiquantitative evidence, considered that order in layer stacking may also result from growth by secondary nucleation if a "structural control" between suc-

cessive sheets exists. The strength of this structural control may depend on environmental conditions of growth leading to more or less ordered structures. This later view is fully supported by our investigations. In type I experiments, we observe on all crystals that whatever the strength of the first dislocation, no interlaced spirals occur, *i.e.*, the structure of the platelet was previously of $1M[0]$ type. Thus the structure of the crystal as a whole will remain unchanged after the adoption of Frank's growth mechanism.

We can say that the same structure was obtained by Yoder and Eugster (1954) during their study of the phlogopite stability range under similar $P–T$ conditions. They did not succeed in distinguishing between $1M[0]$ and $3T[222]$ polymorphs, the two X–ray powder patterns being identical.

In type II runs, various strengths of dislocations and emerging stacking sequences are contributing to give very different growth patterns on {001}, and consequently different surface structures. As no correlation between interlayer stacking angle distributions is observed on the different crystals grown under the same conditions, we deduce that their adopted basic structure was disordered, *i.e.*, $1M,n(120)$, and consequently their initial growth occurs by secondary nucleation. Among the randomly distributed 0°, 120°, 240° stacking angles, we notice that 0° is the more common. If screw dislocations with small **b** appear on this basic structure, short period types like $1M[0]$, $2M_1[2\bar{2}]$, and $3T[222]$ are expected on certain crystals (Figs. 14, 15, 16). Using the above observations, it is now possible to construct the growth sequence of a "representative crystal". During the first stages of growth, following the tri–dimensionnal nucleation at very high supersaturation, the secondary nucleation mechanism is adopted, and leads to a certain basic structure which depends on the environmental conditions of growth. As the supersaturation decreases, the earlier spirals appear on both (001) faces of the crystallite; two different surface structures may eventually be created by the two exposed ledges of the same screw dislocation. With the advance of the prismatic faces, the number of Burgers dislocations increases and we are obliged to consider the structural issues of the successive appearance and simultaneous activity of growth spirals. Successive appearance leads to the fact that a "new" spiral will adopt in its exposed ledge a more or less large part of the ordered stacking sequence of the substrate, and thereby may or may not generate a new type depending upon the previous structure and the strength of the new dislocation. The superposition of polytypes by this mechanism is rendered easy by the phenomenon previously described and shown in Figure 11.

A. BARONNET

Simultaneous activity of several uncooperating spirals will induce, in the more general case, a "patch-work" of different polytypic domains in syntactic coalescence, which may be bounded by fault surfaces. As the supersaturation decreases, a certain part of the above spirals will become cooperative giving a common polytypic structure if core distances $d < 2\pi\rho_c$ with ρ_c as the radius of the critical nucleus for the considered supersaturation. The consequence of such a change will lead once more to a superposition of polytypes. While it is clear that the above considerations are supported by our observations, it does not follow that the growth of each mica crystal is always so complex. In spite of the common occurrence of spiral growth features on (001) faces, we consider that polytypism and especially the appearance of short period polytypes in micas are chiefly governed by secondary nucleation mechanisms. Further work in the line of this paper is required to establish if $2M_1[2\bar{2}]$ in muscovite, $3T[222]$ in phlogopite and muscovite, and $2M_2[1\bar{1}]$ in lepidolite are also surface-nucleated basic structures, these types being found both as "pure" structures and also as "sub" structures in some long-period stacking sequences of natural micas (Ross, Takeda, and Wones, 1966; Takeda, 1971).

REFERENCES

AMELINCKX, S. (1952a) La croissance helicoidale de cristaux de biotite. *C. R. Acad. Sci. Paris.* **234**, 971–973.

—— (1952b) Spiral growth patterns on apatite crystals. *Nature,* **169**, 841–842.

—— (1952c) Growth spirals and their relation to crystal habit as illustrated by apatite. *Nature,* **170**, 760–761.

——, AND W. DEKEYSER (1953) Le polytypisme des minéraux micacès et argileux. *C. R. XIXth Congr. Geol. Int.* 9–22; [*Mineral. Abstr.* **12**, 520].

BASSETT, G. (1958) A new technique for decoration of cleavage and slip steps on ionic crystal surfaces. *Phil. Mag.* **3**, 1042–1025.

BRANDSTÄTTER, M. (1952) Spiralen und Schichtenwachstum an Kristallen aus der Dampfphase I. Mitteilung. *Z. Elektroch.* **56**, 968–972.

—— (1953) Spiralen wachstum an Kristallen aus der Dampfphase II. Mitteilung. *Z. Elektroch.* **57**, 438–444.

DEKEYSER, W., AND S. AMELINCKX (1955) *Les Dislocations et la Croissance des Cristaux.* Masson et Cie Paris.

FRANK, F. C. (1951a) The growth of carborandum: Dislocations and polytypism. *Phil. Mag.* **42**, 1014–1021.

—— (1951b) Capillary equilibria of dislocated crystals. *Acta Crystallogr.* **4**, 497–501.

GRITSAENKO, G. S., AND N. D. SAMOTOYIN (1966) The decoration method applied to the study of clay minerals. *Proc. Int. Clay Conf., Jerusalem, Israel,* **3,** 391–400.

KRETZ, R. (1966) Growth of phlogopite crystals in marble from Quebec. *I.M.A. Pap. Proc. Fifth Gen. Meet.—Cambridge, England,* p. 85–93.

ROSS, M., H. TAKEDA, AND D. R. WONES (1966) Mica polytypes: Systematic description and identification. *Science,* **151,** 191–193.

ROY, R. (1956) Aids in hydrothermal experimentation: II. Methods of making mixtures for both "dry" and "wet" phase equilibrium studies. *J. Amer. Ceram. Soc.* **39,** 145–146.

SELLA, C., P. CONJEAUD, AND J. TRILLAT (1960) Nouvelle méthode d'étude par microscopie électronique de la structure superificielle des faces de clivages d'halogénures alcalins. *IV Int. Kongr. Elektronenmikrosk.* **1,** 508–512.

SMITH, J. V., AND H. S. YODER (1956) Experimental and theoretical studies of the mica polymorphs. *Mineral. Mag.* **31,** 209–231.

SUNAGAWA, I. (1964) Growth spirals on phlogopite crystals. *Amer. Mineral.* **49,** 1427–1434.

TAKEDA, H. (1971) Distribution of mica polytypes among space groups. *Amer. Mineral.* **56,** 1042–1056.

TOLANSKY, S. (1946a) Interferometric studies on mica. *Phil. Mag.* **37,** 453–462.

⸻ (1946b) Further interferometric studies with mica. *Proc. Roy. Soc. London., Ser. A.* **186,** 261–271.

TUTTLE, D. F. (1949) Two pressure vessels for silicate–water systems. *Geol. Soc. Amer. Bull.* **60,** 1727–1729.

VERMA, A. R. (1951) Observations on carborundum of growth spirals originating from screw dislocations. *Phil. Mag.* **42,** 1005–1013.

⸻ (1952) Further observations of growth patterns on silicon carbide (Si-C) crystals. *Phil. Mag.* **43,** 441–446.

⸻ (1953) *Crystal Growth and Dislocations.* Butterworths Sci. Publ., London.

YODER, H. S., AND H. P. EUGSTER (1954) Phlogopite synthesis and stability range. *Geochim. Cosmochim. Acta.* **6,** 157–185.